APRIL 26, 2013

Determining continental crust sources using zircons from Proterozoic Piedmont rocks of central Virginia

Irene Kadel-Harder

GEOL394H

Dr. Aaron Martin and Dr. Phil Piccoli

Abstract

A number of workers have analyzed the meta-igneous rocks from the Goochland terrane in the central Virginia Piedmont Province. Those rock types are gneiss, 'granitoid', amphibolite, and anorthosite. The five rocks sampled for this paper range in age from 1057 to 541 Ma, as determined by U-Pb dating of zircons. The crystallization dates reflect a complex history of orogenic and rifting events starting during the Grenville orogeny and extending through the rifting of Rodinia. This study examines the sources of the igneous rocks during those events in terms of mantle, crustal, or mixed sources.

U-Pb, Lu-Hf, and O isotope data from zircon zones reveal a variety of sources for the rocks. The oldest rock in the terrane, a gneiss, has an isotopic signature of a crustal source. The gneiss has negative εHf values and $\delta^{18}O$ values indicative of a supracrustal sourced melt. The gneiss crystallized during the Grenville orogeny, which would provide a setting for remelting of existing rocks.

The Neoproterozoic granitoids, which were thought to have formed from partial melting of the gneiss, have εHf and $\delta^{18}O$ values indicative of a mantle component in the source of the magma and mixing of a component that was hydrothermally altered at temperatures above 350˚C with a mantle or supracrustal component. High temperature hydrothermal alteration of the source is consistent with the past interpretation that the granitoids formed during a rifting event. Several inherited cores from one granitoid have very similar isotopic signatures to the gneiss, while several inherited cores from the other granitoid have the same εHf values but $\delta^{18}O$ values that suggest a mantle component in the source of the melt.

From the few points collected for the anorthosite, it can be tentatively suggested that the anorthosite has oxygen isotopic signatures very similar to the gneiss. One point has very similar εHf values and $\delta^{18}O$ values to the gneiss. This may be due to incorporation of wall rock as the anorthosite intruded the gneiss at depth, which would affect the isotopic signature of the magma, or a zircon xenocryst from the gneissthat was incorporated into the anorthosite. The three other data points have εHf values like the Neoproterozoic granitoids, suggesting that the anorthosite had a juvenile component in the magma source.

The amphibolite is the youngest rock sampled for this study and is composed of interbedded mafic and felsic layers. The zircon data provides evidence for two different sources for these melts. One source was likely the depleted mantle while the other had components of the depleted mantle and supracrustal material. Future isotopic analyses of these rocks, particularly the anorthosite and the amphibolite, may shed more light on history of the Goochland terrane and the sources of magmas during the supercontinent cycle.

Table of Contents

List of Tables and Figures

Introduction

The formation of continental crust has not been fully explained. Numerous papers have been published over the years postulating that intermediate to andesitic magmas form at oceanic arcs. The magmas are thought to come from subduction related mantle peridotite melting or hydrated mantle peridotite melting followed by fractional crystallization and/or remelting of basaltic arc rocks and delamination of mafic lower crustal material (e.g. Taylor 1967; Pearcy et al., 1990; Rudnick and Fountain, 1995; Tamura and Tatsumi, 2002; Hawkesworth and Kemp, 2006). CITE.

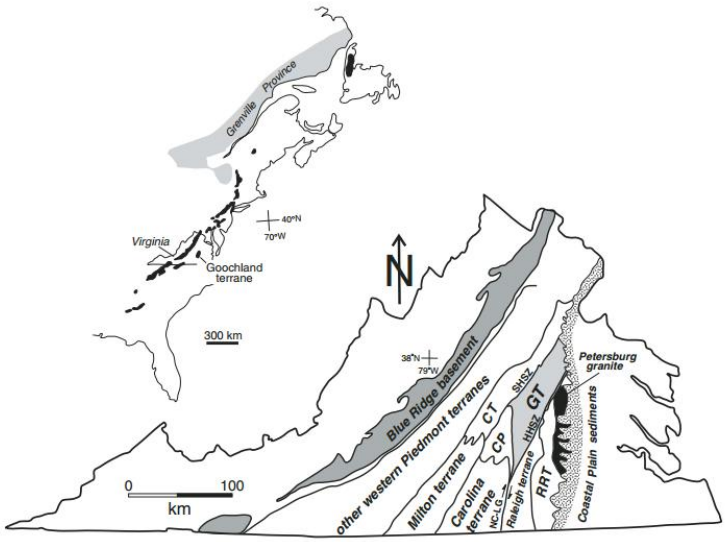

Figure 1. Map from Owens et al. (2010) showing the location of the Goochland terrane on the Eastern Seaboard of the United States and within Virginia. The upper map shows the Goochland terrane in relation to Virginia and other terranes in the Piedmont Province. The lower map depicts geologic areas of Virginia. The Goochland terrane is marked GT and shaded in light gray. HHSZ denotes the Hylas high-strain zone and SHSZ denotes the Spotsylvania high-strain zone.

This thesis addresses two major questions. First, are the sources of continental magmas wholly in the mantle, recycled from existing crustal rocks, or a combination of mantle and recycled crustal rocks? Secondly, are the convergent style orogenic events and later rifting of the Grenville orogeny related to mantle magma, crustal, or combinations of magmas? Analyses of the mineral zircon ($ZrSiO_4$) provide evidence about new continental crust formation, the age of the crust, and the residence time of the magma that would form the continental crust in the crust before it crystallized.

Zircon is an accessory mineral frequently found in igneous rocks. It forms a solid solution with hafnon ($HfSiO_4$) because hafnium and zirconium have the same charge and similar ionic radii. Zircon can contain U, Th, radiogenic Pb, and trace concentrations of REEs and other elements. Zircon can be produced during igneous and metamorphic events. It is frequently used in geologic dating due to its durability and longevity.

Geologic Background

The Goochland terrane is interpreted to be a section of continental crust and is situated within the Piedmont Province of central Virginia (Figure 1) (Owens and Samson, 2004; Owens et al., 2010). It is bordered on the east by the Hylas fault zone and on the west by the Spotsylvania fault. The two oldest rock units within the Goochland terrane formed during the Mesoproterozoic era (1.6 Ga to 1 Ga). The rocks within the terrane underwent granulite facies metamorphism during the Mesoproterozoic, as evidenced by relict granulite assemblages, and amphibolite facies metamorphism during the late Paleozoic (Owens et al., 2010). Some debate surrounds the history of the terrane as a whole; the prevailing interpretation suggests that the

terrane rifted from Laurentia when Rodinia broke up during the Neoproterozoic and later reattached (Owens and Tucker, 2003; Owens et al., 2010).

The State Farm gneiss of the Goochland terrane is exposed in one large, and two smaller, doubly plunging, antiformal domes (Figure 2). The large dome is rimmed by a 1km thick discontinuous layer of the Sabot amphibolite structurally positioned above the gneiss. The State Farm gneiss has a generally granitic mineral assemblage and granitic major and trace elements. The more mafic parts of the gneiss are quartz monzodioritic or quartz monzonitic (Owens and Tucker, 2003). In that study, using Thermal Ionization Mass Spectrometry (TIMS) U-Pb dating of zircons, Owens and Tucker postulated initial crystallization of the granitic protolith sometime within 1057-1013 Ma. These dates are consistent with the youngest crystallization dates of other Grenvillian basement in the Adirondack Mountains and Appalachian Mountains (1030 Ma and 1050 Ma, respectively), suggesting that the State Farm gneiss formed during the Grenville orogeny (Tollo et al., 2004; Owens and Tucker, 2003).

The Montpelier anorthosite lies to the north and west of the largest antiformal dome of State Farm gneiss. Foliation and a mineral-elongation lineation within the surrounding rocks continue through the anorthosite. TIMS U-Pb dating of euhedral, elongate, prismatic zircon grains yielded a crystallization age of 1045±10 Ma (Aleinikoff et al. 1996). This range of dates suggests that the Montpelier anorthosite was emplaced concurrently along with the State Farm gneiss and was also a result of the Grenville orogeny.

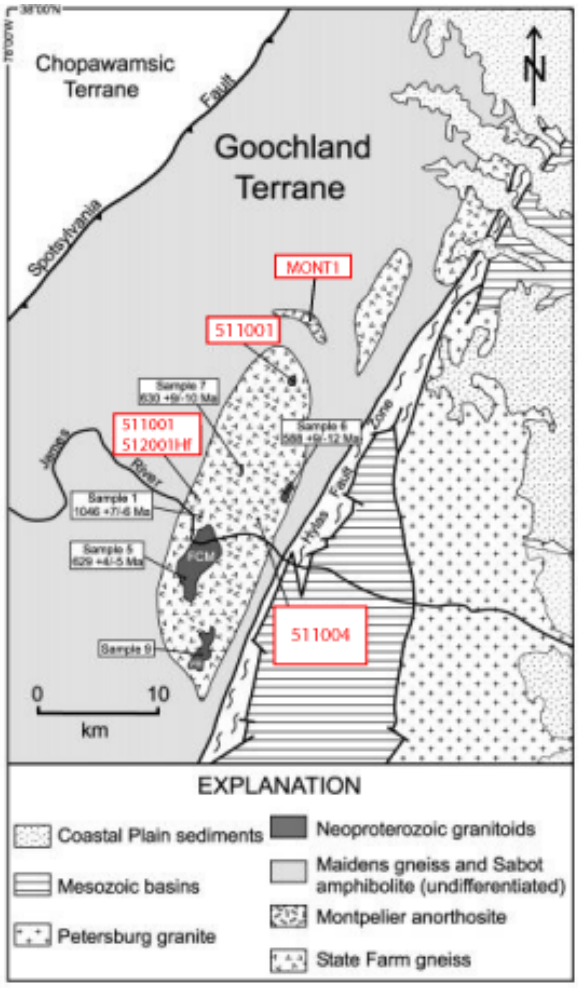

Figure 2. Map showing the locations of units within the Goochland terrane. The boxes describe sample sites and ages from the Owens and Tucker (2003) paper. Four of my samples were taken from the same sites, as noted in red. The fifth was taken from near an anorthosite mine. Modified from Owens and Tucker (2003).

Several granitoid bodies intruded the State Farm gneiss (Figure 2). The granitoids show the compositional characteristics of A-type granites. A-type, or anorogenic, granites form within rift zones and have elevated Ga/Al ratios and high concentrations of high field strength elements such as Nb, Zr, Zn and Y (Owens and Tucker, 2003; Eby, A-type Granitoids). The intruded granitoids have mineral compositions similar to the granitic composition of the gneiss but are more alkaline rich. Some locations show scant deformation while others show foliations and/or lineations. Some samples taken from the granites have abnormally small amounts of quartz (Owens and Tucker, 2003).

As part of a detailed study, Owens and Tucker (2003) imaged zircons from the Neoproterozoic granitoids using standard cathodoluminescence techniques (Figure 2). The zircons contained distinct cores and rims that the authors interpreted to be inherited

Mesoproterozoic cores surrounded by Neoproterozoic rims. Crystallization dates from TIMS U-Pb analyses are ca. 1 Ga for the cores and range from 654 to 588 Ma for the rims. These granites are interpreted to have formed during Neoproterozoic rifting of the terrane. Their source might have been partial melting of the State Farm gneiss or another Grenville aged rock at shallow depths. Due to their Neoproterozoic age and possible rifting induced genesis, the granitoids have been interpreted as comparable to the Robertson River Igneous Suite in the Blue Ridge Province (Owens and Tucker, 2003).

The Sabot amphibolite is a 1km thick sheet that overlies the State Farm gneiss. Lenses of amphibolite are also present in the Maidens gneiss (Owens and Samson, 2004). LA-ICP-MS U-Pb dates from the Martin and Owens abstract (2012) place crystallization at 552±11 Ma. It is interpreted to have formed during the final rifting of Rodinia to open the Iapetus Ocean.

The Maidens gneiss covers most of the Goochland terrane, has a mylonitic texture, has a high K and calc-alkaline protolith composition, and is composed of a heterogeneous assortment of schists and gneisses from various igneous and sedimentary protoliths (Owens et al., 2010). Pegmatitic dikes and sills intruded the biotite gneisses. The entire gneiss unit shows granulite facies metamorphism overprinted by amphibolite facies metamorphism. Using TIMS U-Pb zircon dating, Owens et al. (2010) found dates from around 403 to 386 Ma. The granulite facies metamorphism, which affected the other rocks within the terrane, is dated to around 380 Ma and is interpreted to be the result of the Acadian orogeny. The amphibolite facies metamorphism is interpreted to be the result of the Alleghanian orogeny. The Maidens gneiss is thought to have come from subduction event (Owens et al., 2010).

To summarize the history of the Goochland terrane according to current data and interpretations, the granitic protolith of the State Farm gneiss crystallized sometime within 1057-1013 Ma, as did the Montpelier anorthosite, during the Grenville orogeny. Next the Neoproterozoic granitoids intruded the State Farm gneiss from 654 to 588 Ma during initial rifting of Rodinia. The Sabot amphibolite followed at 552±11 Ma during the final rifting of Rodinia to open the Iapetus Ocean. The Maidens Gneiss is dated from around 403 to 386 Ma. Later, the Acadian orogeny and Alleghanian orogeny deformed the rocks of the terrane. Where the Goochland terrane was located during its later history is the subject of debate. The prevailing interpretation suggests that the terrane rifted from Laurentia when Rodinia broke up during the Neoproterozoic and later reattached (Owens and Tucker, 2003; Owens et al., 2010).

Petrography

The State Farm gneiss contains quartz, potassium feldspar, plagioclase feldspar, biotite, garnet, and titanite, and can include hornblende and small amounts of apatite, magnetite, epidote, and zircon (Figure 3) (Owens and Tucker, 2003). The feldspars show some alteration to clay. A strong foliation is present. The zircon grains that are visible seem to occur near the biotite and

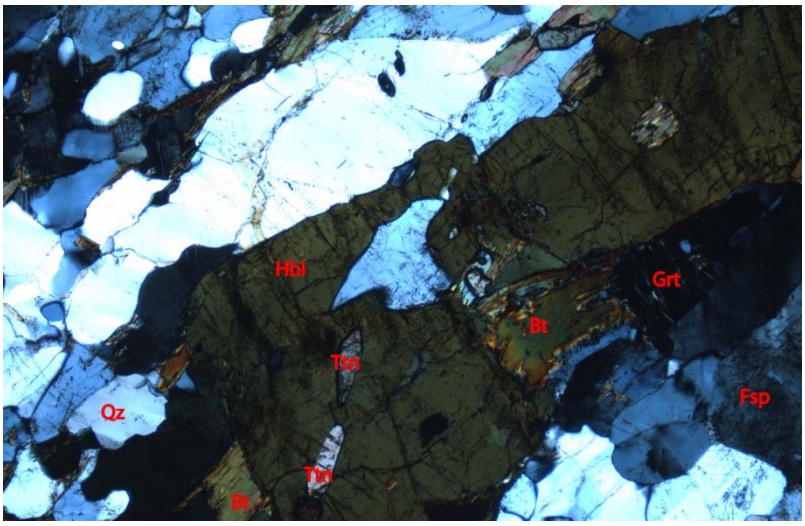

Figure 3. Photomicrograph image of the State Farm gneiss in cross polarized light.

hornblende, which are the most obvious markers of the foliation.

The zircons in the State Farm gneiss are elongate, euhedrally prismatic crystals with a small amount of rounding on the tips and faces. This suggests igneous formation with later alteration by a metamorphic event. Cathodoluminescence images show oscillatory zoning (Owens and Tucker, 2003).

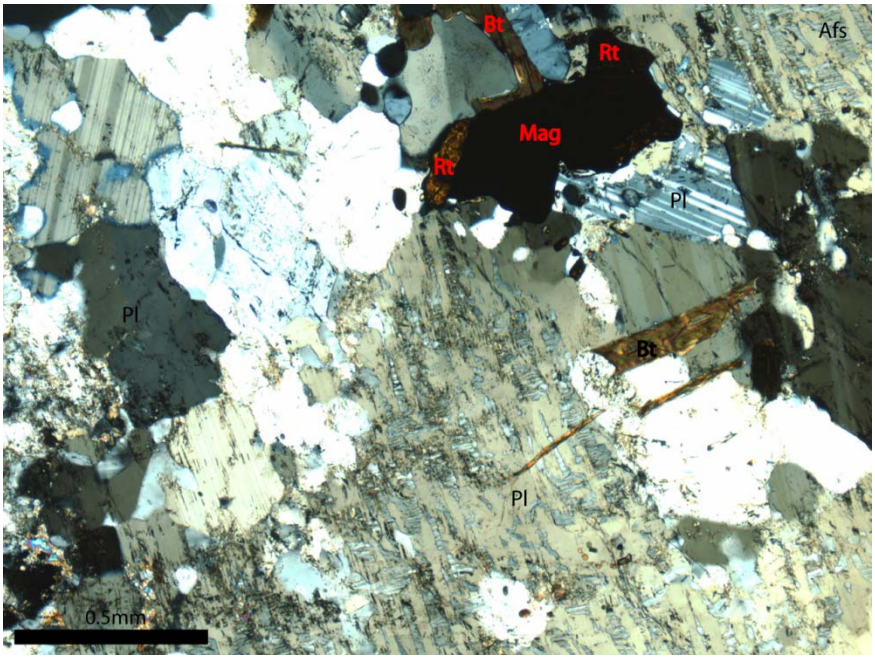

Figure 4. Photomicrograph image of the Montpelier anorthosite in cross polarized light. The plagioclase shows antiperthitic texture

Foliation and a mineral-elongation lineation within the surrounding rocks continue through the anorthosite (Alienikoff et al., 1996). The Montpelier anorthosite consists of two textural varieties. One variety is coarse, unfoliated, and contains antiperthitic andesine, which is plagioclase feldspar with exsolution lamellae of potassium feldspar (Nesse, 2000). This textural variety contains pyroxene altered to pseudomorphs of uralitic amphibole, which is fine-grained, light-colored amphibole. This variety also contains quartz, biotite, chlorite, ilmenite, rutile, garnet, titanite, biotite, apatite, zircon, muscovite, prehnite, anatase or leucoxene, and weathering products. The other variety of anorthosite is a white, foliated and lineated, fine-grained, granoblastic meta-anorthosite (Aleinikoff et al., 1996). Nelsonite, a rock comprising apatite, ilmenite, and possibly rutile, is found within the anorthosite in masses with diameters of several centimeters (Alienikoff et al., 1996).

A thin section was cut to cross a contact between magnetite and andesine. There is a well-defined corona around the magnetite consisting of rutile, titanite, biotite and intergrown quartz, and garnet. The plagioclase displays varying textures throughout the thin section. The most easily characterized texture is myrmekite. Other areas display antiperthitic texture with exsolution lamellae of alkali feldspar. Some small plagioclase grains show polysynthetic twins; the large crystals in the thin section show no twinning. The plagioclase displays a sieve texture where it has grown around the other crystals.

The mineralogy of the Neoproterozoic granitoids is similar to that of the State Farm gneiss. This rock is comprised of quartz, potassium feldspar, plagioclase feldspar, biotite, garnet, amphibole, and magnetite. The rock can also contain allanite, fluorite, and clusters of biotite and amphibole. The amphiboles and biotite are dark colored in thin section, which is likely due to high Fe content (Owens and Tucker, 2003).

Sample 511001 (which will now be referred to as granitoid A) from a Neoproterozoic granitoid, shows a strong lineation but is not foliated in hand sample. It is more coarse-grained than the State Farm gneiss, but finer grained than the other Neoproterozoic granitoid. Sample

511004 (which will now be referred to as granitoid B) is the other granitoid; it has very large

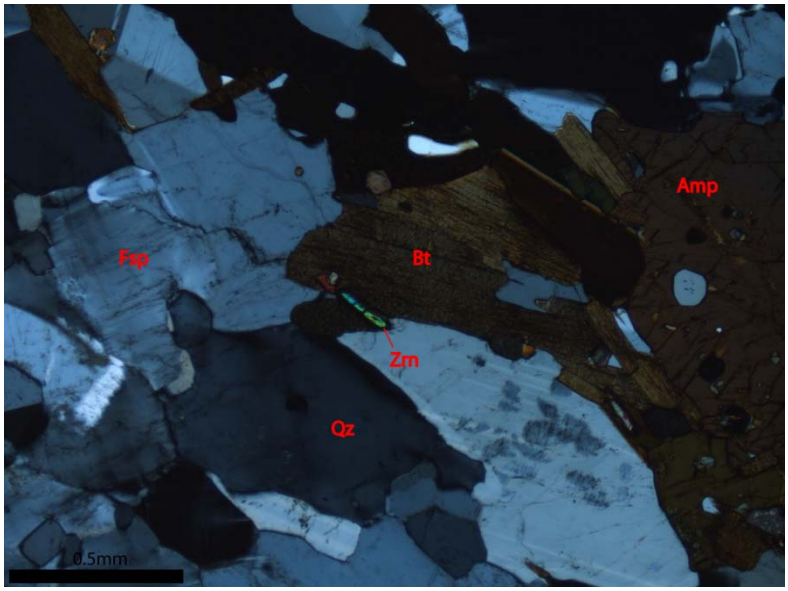

Figure 5. Photomicrograph image of granitoid A in cross polarized light. The bright elongate grains are zircons.

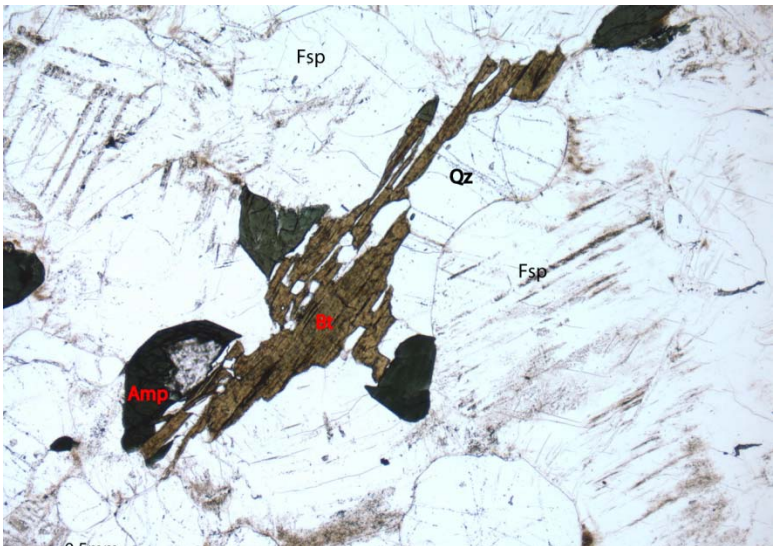

Figure 6. Photomicrograph image of granitoid B in plane polarized light. The amphibole and biotite are dark colored, likely due to high Fe content.

grains and a less obvious mesoscopic foliation. The feldspars are altered to clay minerals in some grains. Quartz shows undulatory extinction.

Owens and Tucker (2003) analyzed zircons from the Neoproterozoic granitoids and found analytical discordance for their U-Pb dates. They posited the discordant values resulted from two different age populations of zircons. Cathodoluminescence images of their samples showed zircon overgrowths with fine scale zoning, which they interpreted as Neoproterozoic igneous crystallization. The event causing this igneous crystallization was TIMS U-Pb dated to 630-588 Ma. The smaller cores were thought to be inherited Mesoproterozoic grains (Owens and Tucker, 2003).

The Sabot amphibolite thin section was cut to show the contact between the amphibolite

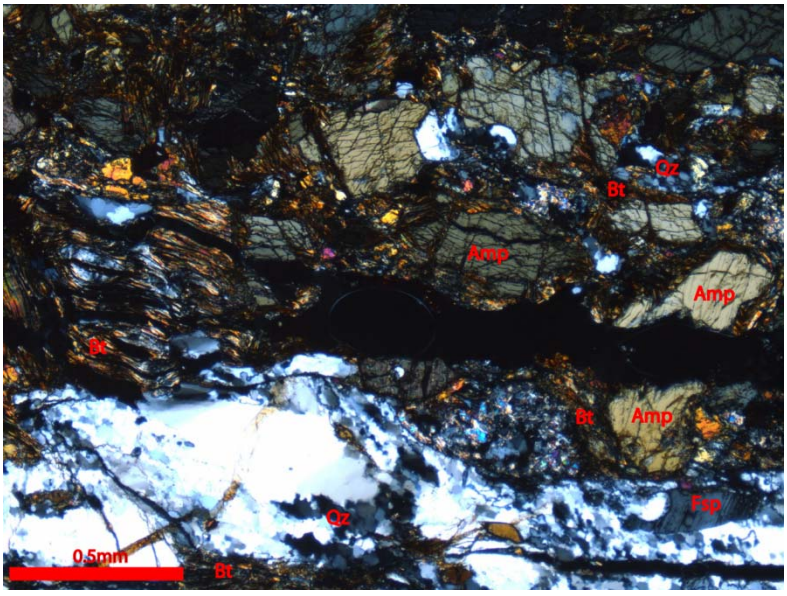

Figure 7. Photomicrograph image of the Sabot amphibolite in cross polarized light. The dark crack in the middle of the image is the contact between the amphibolite and the more felsic region in the thin section.

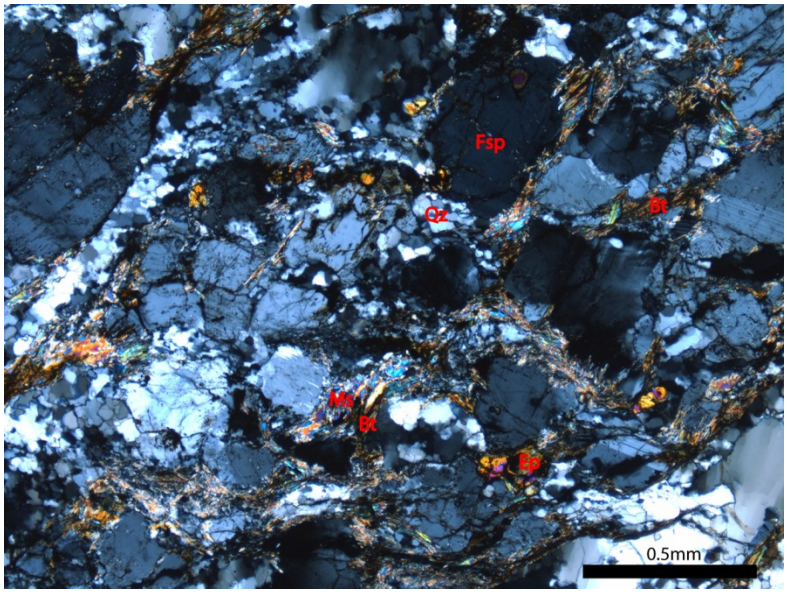

Figure 8. Photomicrograph image of Sabot amphibolite in cross polarized light. The felsic region is composed of feldspars, quartz, biotite, and small epidote grains. Recrystallized quartz and bent biotite crystals are evidence of deformation.

and a more felsic section of the rock. Amphiboles, titanite, deformed biotite, and epidote are found in the amphibolite section. Feldspars, recrystallized quartz, deformed biotite, and epidote comprise the felsic section.

Isotopic Geochemistry Background

Lutetium-Hafnium System

Lutetium (Z=71) is the heaviest rare earth element. It has two stable isotopes, ^{175}Lu and ^{176} Lu, which have abundances of 97.4% and 2.6%, respectively. ^{176}Lu is much less abundant because it decays either through electron capture to ^{176}Yb or through β-decay to ^{176}Hf followed by γ emission to a ground state. The amount of ^{176}Yb created is so small that it is negligible (Dickin, 1997). ^{176}Lu decaying to ^{176}Hf has a half life of ~37.2 Ga (Kemp and Hawkesworth, unpublished chapter). The concentration of ^{176}Hf is commonly divided by the concentration of ^{177}Hf, a stable isotope (Dickin, 1997).

Hafnium is more incompatible than Lu during melting of spinel and garnet peridotite in the mantle; that is, it preferentially partitions into the melt. The residue is enriched in Lu, leading to a higher Lu/Hf mantle and a lower Lu/Hf crust. This then leads to a higher ^{176}Hf/^{177}Hf ratio in the mantle and a lower ^{176}Hf/^{177}Hf ratio in the crust, with time.

The charge and atomic radius similarities between Zr (Z=40) and Hf (Z=72) facilitate substitutions of Hf into the crystal structure of zircon crystals for Zr. Due to hafnium's role in the crystal structure, it is unlikely to be replaced by other atoms that could otherwise alter the Lu/Hf ratios (Dickin, 1997). Hafnium can be present at weight percent concentrations within zircons so measurements of the Lu/Hf ratio can generate ^{176}Hf/^{177}Hf ratios and Hf model ages (Kemp and Hawkesworth).

Zircons usually have a Lu/Hf ratio less than 0.002, which increases the accuracy of age calculations. The low Lu/Hf ratio also means that zircons retain close to the initial ^{176}Hf/^{177}Hf ratios at the time of crystallization (Kemp and Hawkesworth, unpublished chapter). That initial ratio is used to calculate a Hf model or crustal residence age, which gives the time since the source of the magma from which the igneous zircon crystallized separated from the depleted mantle. Increasing equipment precision has led to measurement of the Hf isotopes within growth zones in zircons, which can depict changing isotopic composition of the melt and the growth history of the zircon. The Hf model age, when used in combination with U-Pb dates for zircon crystallization, can give estimates of when continental crust formed (Kemp and Hawkesworth; Kinny and Maas, 2003).

Uranium-Lead System

Uranium (Z=92) is a heavy element that is incompatible during melting, concentrates in the melt, and is therefore found in high concencentrations in the silicate-rich magmas that ultimately crystallize to yield granites (Faure, 1986). Uranium has three isotopes, all of which are radioactive: ^{238}U, ^{235}U, and ^{234}U. These nuclides decay through two decay chains (^{234}U is a daughter of ^{238}U) to form ^{206}Pb and ^{207}Pb, respectively. Pb has two other isotopes; ^{208}Pb is formed from the radioactive decay of thorium and ^{204}Pb is stable and nonradiogenic, so it is used as a reference isotope.

Due to similarity between the ionic radii of U^{4+} and Zr^{4+}, the crystal structure of zircon can accept significant uranium, which is found in the 10-100ppm concentration range. Zircon

does not incorporate significant Pb into its crystal structure during crystallization. This leads to a high initial U/Pb value (Parrish and Noble, 2003).

U-Pb isotopes begin recording during the high temperatures at which zircon crystallized, whether that crystallization happened during igneous formation or metamorphic recrystallization (Kemp and Hawkesworth, unpublished chapter). The crystallization ages are determined by plotting the $^{238}U/^{206}Pb$ data and $^{235}U/^{207}Pb$ data on a concordia diagram. The $^{207}Pb/^{206}Pb$ ratio can be used to calculate a date for the zircon. This ratio is used because it was not affected by lead loss from the crystal (Parrish and Noble, 2003; Faure, 1986).

Oxygen system

Oxygen (Z=8) has three stable isotopes: ^{16}O, ^{17}O, and ^{18}O. 99.63% of all oxygen isotopes are ^{16}O, followed by ^{18}O with 0.1995%, and ^{17}O with 0.0375%. The isotopic composition is written as the ratio $^{18}O/^{16}O$ and is compared to SMOW (Standard Mean Ocean Water) or VSMOW (Vienna Standard Mean Ocean Water). Values above the $\delta^{18}O$ SMOW concentrations are positive and enriched in ^{18}O; values below SMOW are negative and depleted in ^{18}O (Faure, 1986).

Zircon maintains the approximate oxygen isotope ratio of the magma from which it formed; however, some fractionation does occur between the zircon and the melt. Zircons that have reached equilibrium with "pristine" mantle-derived melts have $\delta^{18}O$ values of $+5.3 \pm 0.6‰$ at 2SD. Mafic melt values increase by +0.5‰ and silicic derivatives increase by +1.5 to +2‰. $\delta^{18}O$ values above +6‰ represent a ^{18}O enriched supracrustal (contact with meteoric water) component in the magma. Sedimentary rocks have values of +10 to +30‰ and weathered volcanic rocks have values of +20‰. Reworked hydrothermally-altered crustal magmas have depleted $\delta^{18}O$ values (Kemp and Hawkesworth; Valley, 2003).

Hypothesis

The magmas that formed the five igneous rocks came only from crustal sources. To test this hypothesis, I performed isotope analyses for oxygen, Lu-Hf, and U-Pb on separated zircons to test the hypothesis regarding the sources of the magmas.

Methods of Analysis

As part of this work, I chose a group of igneous rocks from the same tectonic region with previously published zircon crystallization ages from TIMS U-Pb analyses of igneous zircon grains. I have examined the CL images to find recrystallized zones in the zircon grains. I have separate and mounted zircons from the five rocks for three types of isotopic analyses. I have collected CL images of designated zircons to insure that the isotope analyses are performed on the igneous sections of the grains, not the metamorphic or inherited sections. I have gathered oxygen isotope data to compare with accepted mantle oxygen ratios. I have gathered Lu-Hf isotope data to calculate the model age for separation of the source(s) of magma from the mantle. I have gathered U-Pb data to interpret crystallization ages for cores, mantles, and rims of the zircons.

Thin Sections

Thin section billets of the five samples were cut during June in the Geology department rock cutting room. Dr. Aaron Martin assisted with saw training. The radial saw was used to cut the billets and a previously cut billet returned by the thin section manufacturer served as a

template. The billets were approximately 44mm by 24mm by 20mm. The thickness of the billet was not considered critical because it would be filed down later.

Two of the billets were held together by rubber bands due to their fragile nature. The anorthosite cracked while being cut. The Sabot amphibolite was very fragile and cracked into pieces while it was being cut. These samples were impregnated with epoxy when the mounts were made.

Zircon Separation

Zircons were separated from the rocks using several steps. First, the rocks were washed by hand with water and a scrub brush, then crushed using a steel mortar and pestle in the rock cutting room. They were sieved using 400 micron nylon mesh, then hand panned to remove clay and silt sized particles. Next the sand was magnetically separated using a hand magnet and the Frantz Magnetic Separator. Samples were separated at currents ranging from 0.50 A to the maximum amps setting on the machine, approximately 2.25 A.

The nonmagnetic portion was then separated using methylene iodide, a dense liquid. Methylene iodide, or diiodmethane (H_2I_2), has a specific gravity of about 3.31g/cc and dissolves in acetone (Nesse, 2000). Zircon grains are denser than methylene iodide and usually sink to the bottom of the liquid. The bottom layer of methylene iodide was frozen using liquid nitrogen and the top portion was poured off and filtered with filter paper and acetone to remove the methylene iodide. The solid methylene iodide was melted using warm water and the denser grains were filtered using acetone and filter paper. These 'float' and 'sink' grains were then dried under a heat lamp and stored separately until the 'sinks' were picked using tweezers for mount making.

This method of dense liquid separation was used for all of the samples. The Montpelier anorthosite 'sinks' were mostly rutile grains with few zircons, so methylene iodide in a separatory funnel was also used to isolate the zircons.

Using a stereoscopic microscope, the zircons were picked from the other dense grains with tweezers and placed onto a piece of tape used to corral acceptable grains. There was a sampling bias toward colorless, prismatic, elongate, euhedral grains because these grains are most likely to be zircons and not rutile, free of inclusions, and of igneous origin. These are also most likely to be igneous zircons, which would provide data about initial igneous crystallization, rather than later metamorphic (re)crystallization. Colored, rounded, equant grains with inclusions are more likely not zircon or zircons that formed during metamorphic events after crystallization.

Three mounts were created for small, medium, and large zircon grains. All grains were placed within 5mm of the center of the mount on another piece of tape. The standards provided by the University of Wisconsin-Madison Secondary Ionization Mass Spectrometry (SIMS) lab and the University of Arizona-Tucson Laser Ablation Inductively Coupled Plasma Mass Spectrometry (LA-ICP-MS) lab were placed first in the center of the mount and the zircons from my samples were placed around them. Epoxy was poured over them and allowed to cure for six days, then was detached from the tape and cleaned with ethanol to remove tape residue.

The mount was then ground using wet 2000 grit (approximately 9.6 micron) sandpaper to reach a depth of 25-35% of the zircon grains, wet 2500 grit (approximately 7.8 micron) sandpaper to reach a depth of 50% of the zircon grains, and wet 3000 grit (approximately 6.6 micron) sandpaper on a glass plate for two minutes. The mounts were polished on wet 5 micron grit paper on a glass plate for two minutes, wet 3 micron grit paper on a glass plate for 10 minutes, and wet 1 micron grit paper on a glass plate for 10 minutes.

The mounts were photographed using the petrographic microscope camera and accompanying software. The images were imported into Adobe Illustrator and the zircons were labeled with the sample number and an additional identifier, either a number for the unknowns (i.e. 511005-1) or a letter for the standards (i.e. MT-A). The mounts were then sent to Dr. John Valley at the University of Wisconsin-Madison SIMS lab to be checked for any issues that would prohibit using the ion probe, such as surface relief or a lack of planarity.

Imaging

The Electron Probe Microanalyzer (EPMA) was used to make cathodoluminescence (CL) and backscatter electron (BSE) images. These images were used to find the igneous parts of the zircon grain and avoid cracks, inclusions, and inherited and metamorphic parts of the grains. A carbon coat was applied to samples before they were inserted into the EPMA. Dr. Martin and Dr. Piccoli assisted with training and general oversight. After inserting the sample into the EPMA, the focus was tested and set for the machine. For each sample the BSE and CL contrast and brightness were checked to insure that the image would not be too bright or too dark. Then the sample number and contrast information – either high, low, or normal – were entered and the image was acquired over a 2 minute period. The EPMA was set to the smallest beam diameter possible, a 20 nAmp current, and a 15kV voltage. Figure 9 includes a BSE and CL image of two grains from the Sabot amphibolite.

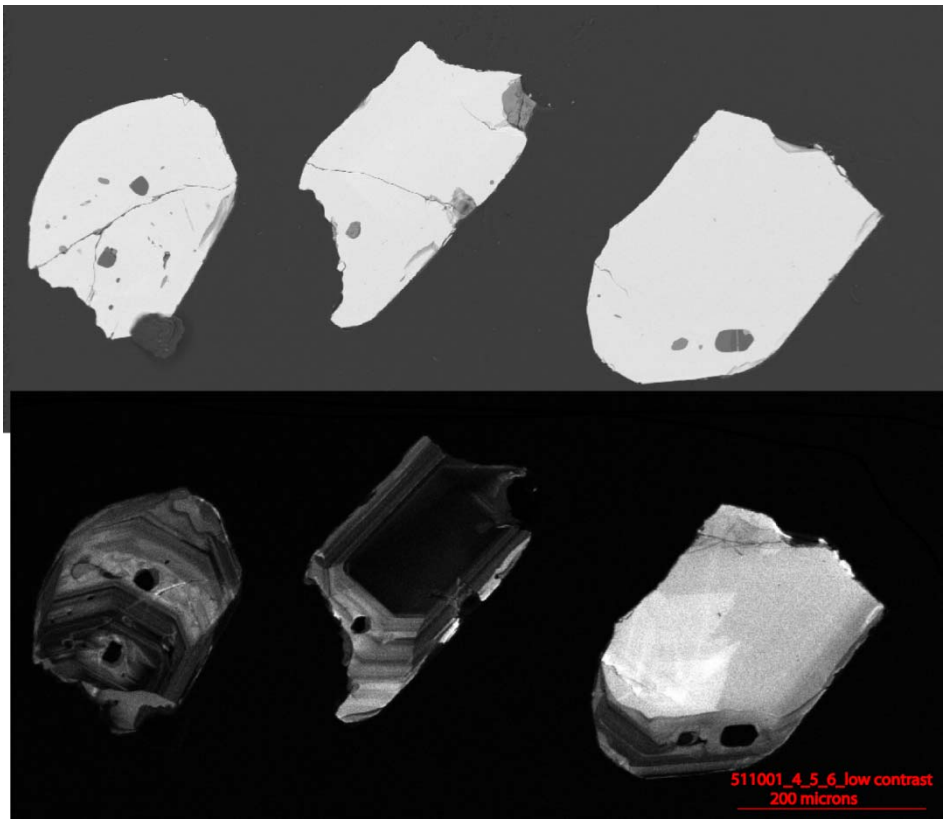

Figure 9. Backscatter electron (above) and cathodoluminescence (below) images of zircons from Neoproterozoic granitoid A. Zones and inclusions are visible in all three grains. Darker cores are recognizable in the left and center grains. Owens and Tucker (2003) presented U-Pb data from zircons that gave two zircon age populations. Inherited cores were dated to ~1000Ma while younger rims of the zircons were dated to 654 to 588Ma. The brighter, massive part of the right zircon creates ambiguity about its crystallization history.

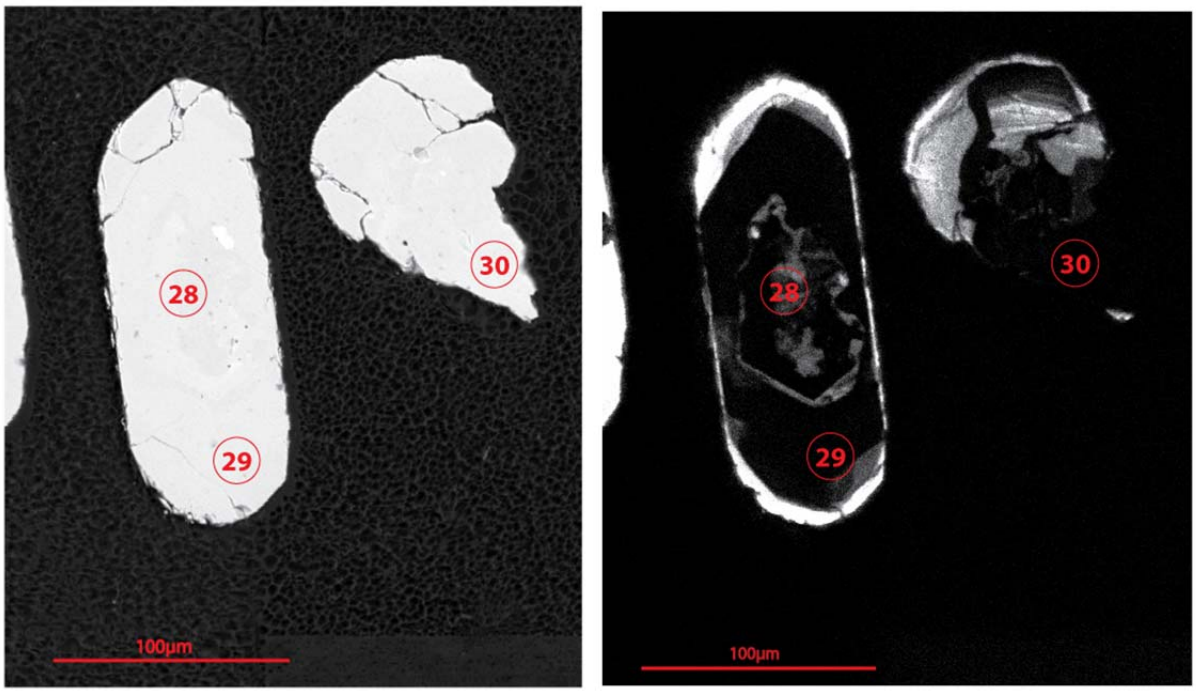

Figure 10. BSE image (left) and CL image (right) of two grains from the Sabot amphibolite. Spots for analysis are marked in red and numbered. The diameter of the circles is 30 microns, which is the beam size used for oxygen isotope analyses and some of the U-Pb and Lu-Hf analyses.

Results

Using the transmitted light photomicrograph, CL, and BSE images, I identified spots for analysis in the zircons that were not in inclusions or fractures. Most spots were in the igneous growth zones of the grains. Figure 10 includes numbered BSE and CL images of two grains from the Sabot amphibolite. A core is visible in the left zircon in both BSE and CL images. Spot 28 is located within the core and spot 29 is located in a dark midsection of the grain. The right grain is fractured and spot 30 is situated in an area of darkness. It would appear that the dark area is a core or midsection of the grain.

SIMS work was completed at University of Wisconsin-Madison on the CAMECA IMS-1280 in Dr. John Valley's lab. Data was compared to VSMOW and Kim-5 was used as a standard. Sample spots were 40 microns wide. Split stream LA-ICP-MS work was done at Washington State University on the Finnigan Element2 HR-ICP-MS and Finnigan Neptune MC-ICP-MS in Dr. Jeff Vervoort's lab. Dr. Martin and I were assisted by his graduate student, Chris. We obtained simultaneous U-Pb and Lu-Hf data per spot. Sample spots were 30 or 40 microns wide, depending on the size of the zircon grain. Standards used were NIST glass, Plesovice, and FC-1. Some of the analyses hit multiple zones within the zircons, which resulted in weak signals in the Lu/Hf data and/or multiple peaks in the U/Pb data. Lu/Hf data for an analytical run were initially excluded if the graph of the data was not one distinct peak or had low signal.

The U/Pb data for all samples were cut at 100 hits per spot. Some analytical runs were cut at smaller numbers of hits per spot to constrain the data to one zone within the zircon. This usually led to increased one sigma absolute uncertainty. The spreadsheet provided by Washington State University calculated the slopes of the $^{206}Pb/^{238}U$ data points, $^{207}Pb/^{235}U$ data

points, and $^{207}Pb/^{206}Pb$ data points. I used the $^{207}Pb/^{206}Pb$ age as the crystallization date of the spot.

There are a variety of sources of error. Random, or measurement, error comes from the measurements the mass spectrometer makes. During data reduction the software quantifies these errors. Other random errors may come from uncertainties in the measurements made with the machines, both on the sample zircons and the standards. Systematic errors may come from uncertainties on the decay constants, uncertainties in the isotopic values for the standards, and the composition of common Pb.

Systematic error could also be generated by large relief on the grain mount surfaces as a result of polishing. High relief (10-40μm) creates topographic effects that enrich $\delta^{18}O$ values by as much as +4‰. We have addressed this possible source of error by polishing the mounts as little as possible, using very fine sandpaper, and following the directions of John Valley. All grain mounts were sent to his facility and the relief was declared acceptable (Kita et al., 2009). For the rest of the paper, error on data values will not be explicitly stated but will be represented on graphs with error bars of standard error.

Table 1 displays the maximum, minimum, and average data values for the five different rocks. Data points were included if the $^{207}Pb/^{206}Pb$ ages were slightly below, at, or above the published ages for the rocks. This accounts for possible lead loss of the samples. Data points were excluded if the $^{207}Pb/^{206}Pb$ ages were much higher or lower than the published age and particularly if their ages suggested they could have been formed during a metamorphic event.

47 spots were analyzed for the State Farm gneiss. Five points were excluded because their $^{207}Pb/^{206}Pb$ ages were greater than 1100Ma. All of those spots have $\delta^{18}O$ data, but only 38 have U-Pb and Hf data. U-Pb crystallization dates ranges from 928 to 1100Ma. The State Farm gneiss has an average crystallization date of 1029Ma with a 1σ absolute error of 33Ma, which is consistent with Owens and Tucker (2003). The $\delta^{18}O$ values range from 9.69 to 6.93‰ and have an average 2σ error of 0.14‰.

20 spots were analyzed for the Montpelier anorthosite. More than 20 spots were identified for analysis, but the zircon grains were small, frequently fractured, contained inclusions, and had low Pb concentrations. These factors made it difficult to collect useable data. Six samples have hafnium values, but two of these samples were excluded because their crystallization ages were 699 and 732Ma. This reduces the anorthosite's data to 4 points. The $\delta^{18}O$ values range from 7.60 to 8.40‰ and have an average 2σ error of 0.26‰.

41 spots were analyzed for granitoid A. Most growth dates to around 1000Ma and around 620Ma. These dates correspond to the ~1000Ma and 654-588Ma U-Pb crystallization ages reported by Owens and Tucker (2003). 11 spots with crystallization dates that fell outside of the established dates were excluded. Regions that crystallized around 1000Ma are grouped as either 'inherited cores' or 'old regions', which refer to ~1000Ma zones that are not cores. The $\delta^{18}O$ values for the inherited cores average 7.56‰ with an average 2σ error of 0.21‰, the $\delta^{18}O$ values for the old regions average 6.76‰ ± 0.28‰, and the regions dated around 620Ma average 6.54‰ ± 0.21‰.

48 spots were analyzed for granitoid B. Most growth dates to around 1000Ma and around 620Ma, which correspond to the U-Pb crystallization ages reported by Owens and Tucker (2003): ~1000Ma and 654-588Ma. 9 analyzed spots that did not fall into those age populations were excluded because they formed outside of the two known zircon forming events. The ~1000Ma points were grouped as either 'inherited cores' or 'old regions'. The $\delta^{18}O$ values for

the inherited cores average 4.31‰ with an average 2σ error of 0.27‰, the $\delta^{18}O$ values for the old regions average 2.81‰ ± 0.28‰, and the regions dated around 620Ma average 4.39‰ ± 0.26‰.

39 spots were analyzed for the Sabot amphibolite. 10 spots were excluded because the $^{207}Pb/^{206}Pb$ ages were below 500Ma. The average crystallization age is 561Ma ± 44.1Ma, which concurs with 552±11 Ma, the date published in Martin and Owens abstract (2012). The $\delta^{18}O$ values range from 5.57 to 9.33‰ ± 0.21‰.

Figure W is a plot of the $\delta^{18}O$ data for the State Farm gneiss and the Neoproterozoic granitoids versus the sample number. The State Farm gneiss data plot around or above 6.40‰. The highest value is 9.69‰. Granitoid A has values ranging from 6.21‰ to 8.29‰. The inherited cores range from 6.51‰ to 9.69‰ and the two 1000Ma regions plot at 6.65‰ and 6.86‰. The data for the regions of the granitoid that crystallized at 620Ma range form a tight cluster between 6.21‰ and 7.05‰.

Granitoid B has a much wider spread of $\delta^{18}O$ values, with values falling from 1.78‰ to 6.56‰. The inherited cores range from 3.58‰ to 4.52‰ and the 1000Ma regions plot from 1.78‰ to 4.91‰. The regions within the zircons that crystallized around 620Ma plot from 1.79‰ to 6.56‰.

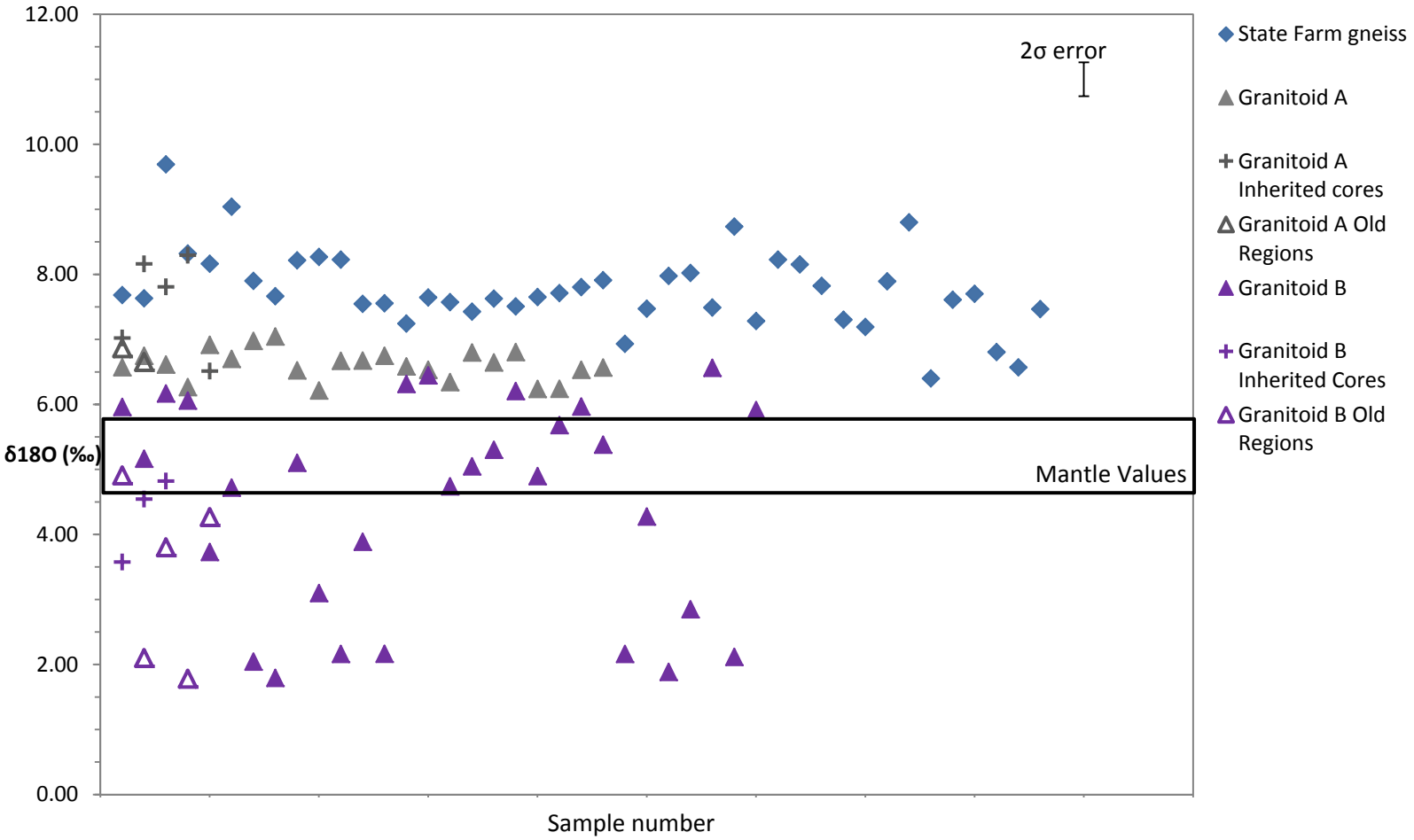

Figure 11. Graph of $\delta^{18}O$ values for the State Farm gneiss and Neoproterozoic granitoids A and B. The $\delta^{18}O$ range for the mantle is outlined in black and is from Kemp and Hawkesworth.

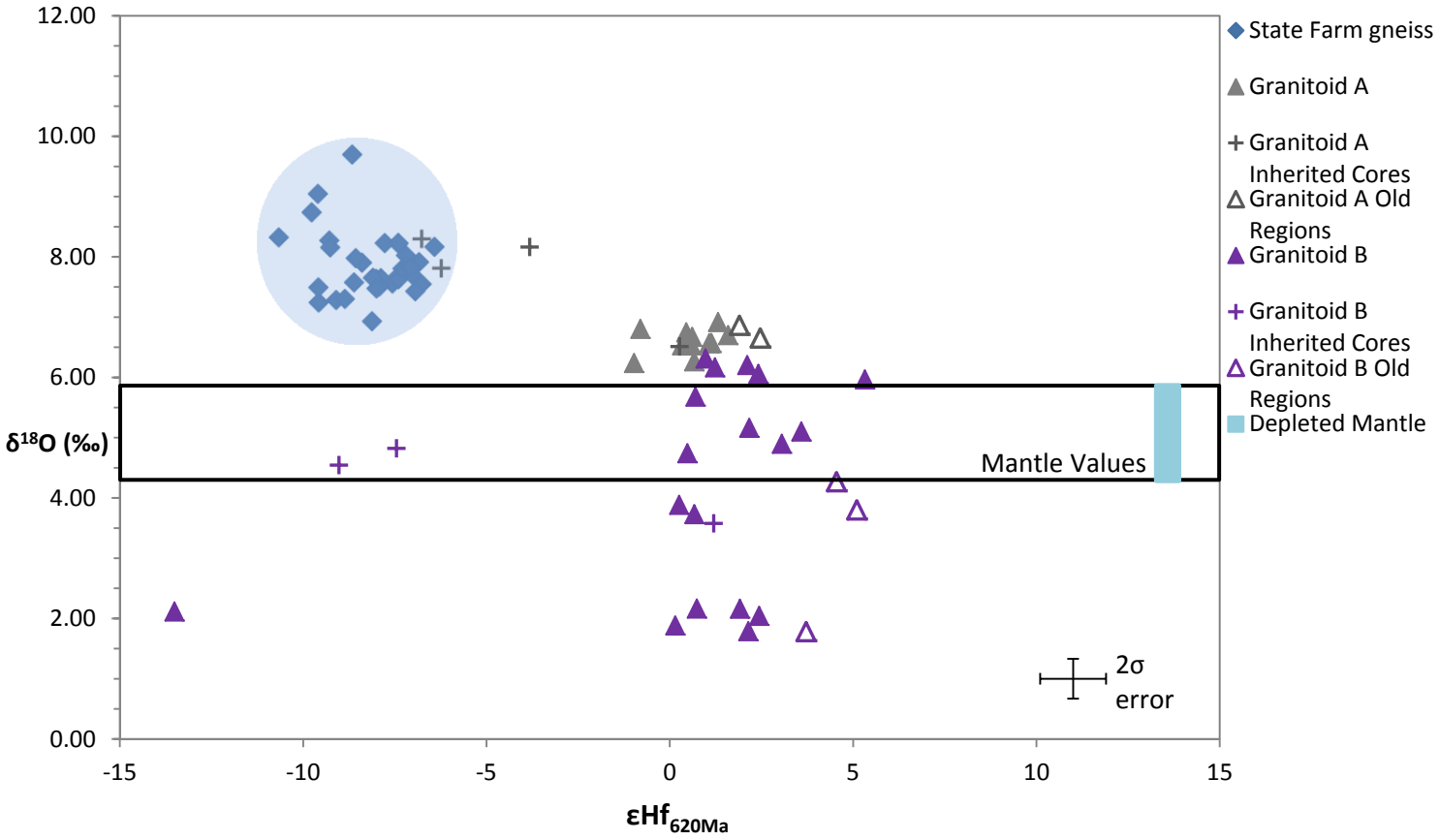

Figure 12. Graph of $\delta^{18}O$ values compared to the epsilon hafnium values of the State Farm gneiss and granitoids A and B at 620Ma.

For the εHf calculations, Chondritic Uniform Resevoir (CHUR) values for today were taken to be $^{176}Hf/^{177}Hf = 0.282785$ and $^{176}Lu/^{177}Hf = 0.0336$ from Bouvier et al. (2008). The decay constant was 1.867×10^{-11} yr^{-1}, from Scherer et al. (2001). The $^{176}Lu/^{177}Hf$ value of the crust throughout time was assumed to be 0.015 (e.g. Griffin et al., 2004). Depleted mantle (DM) values are taken to be $^{176}Hf/^{177}Hf = 0.283255$ and $^{176}Lu/^{177}Hf = 0.038512$, from Vervoort and Blichert-Toft (1999). All of the data for each rock was assigned a fixed age for the εHf calculations based on the ages determined by more precise U-Pb dating. The State Farm gneiss was assumed to have crystallized at 1050Ma, the Montpelier anorthosite at 1040Ma, and the Sabot amphibolite at 560Ma. Because the Neoproterozoic granitoids have inherited regions and younger regions, the εHf values were calculated with assumed 1000Ma and 620Ma crystallization dates, respectively.

Figure 12 is a graph of $\delta^{18}O$ versus εHf at 620Ma. The State Farm gneiss and granitoids' inherited cores and older regions have been recalculated to find the εHf at the time when the granitoids crystallized. The State Farm gneiss clusters between -11 and -6, as do four ~1000Ma cores from granitoids A and B. A third ~1000 core from granitoid A is situated around -8ε units. The remaining inherited cores, older zircon regions, and the regions that crystallized at 620Ma range from -0.8 to +5.. One point from granitoid B plots at -13.5 and has higher measured amounts of $^{176}Hf/^{177}Hf_0$ and $^{176}Lu/^{177}Hf_0$ than many other analytical spots from granitoid B.

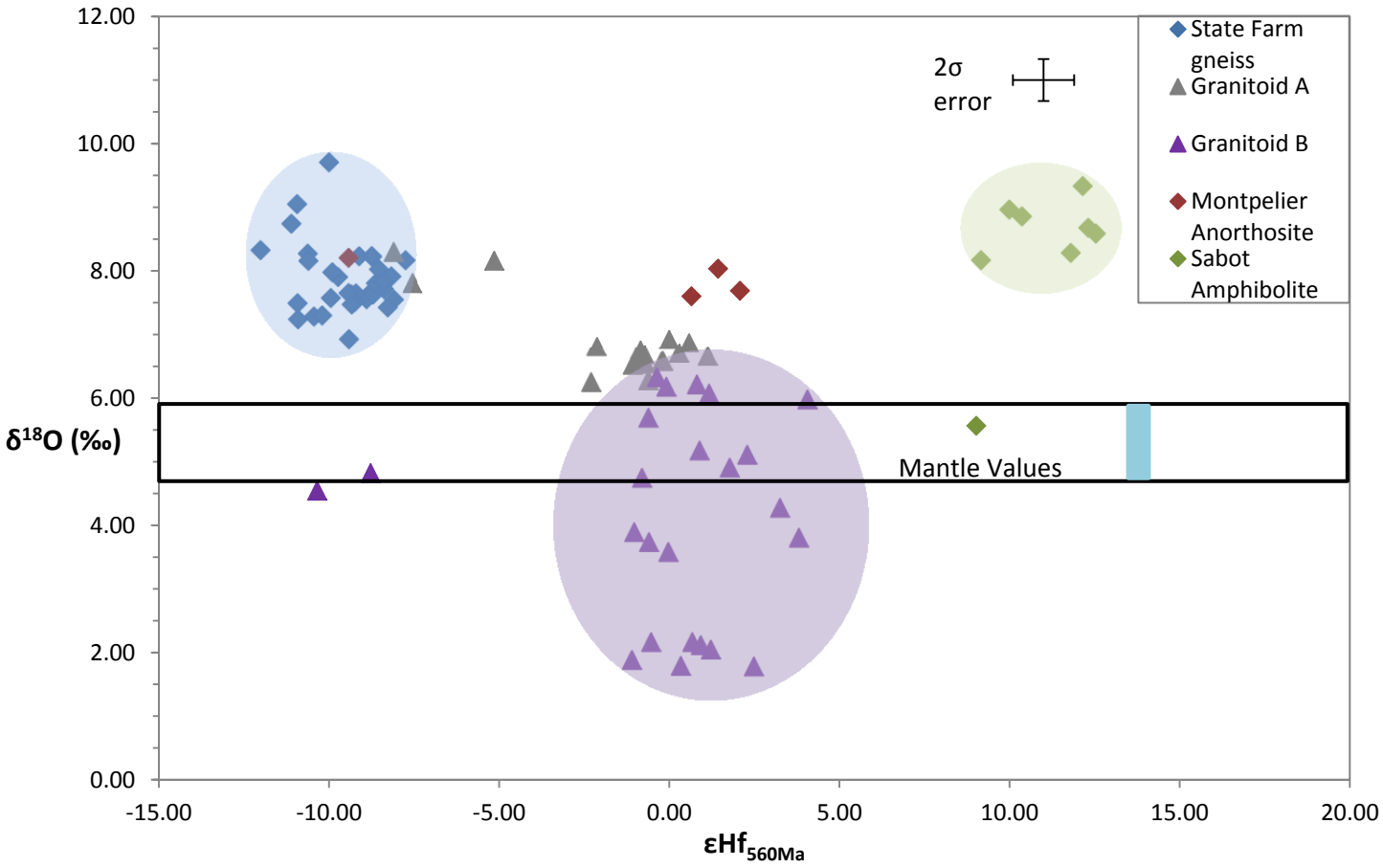

Figure 13. Graph of $\delta^{18}O$ values compared to εHf of all five rocks calculated at 560Ma.

Figure 13 is a graph of $\delta^{18}O$ versus εHf at 560Ma, the time of crystallization for the amphibolite. The gneiss, anorthosite, and granitoids plot from about -12 to +4. The Monpelier anorthosite has only four data points. Three are clustered around +1.4 and 7.7‰. The other point falls at -9.43 and 8.20‰, which is within the range of the State Farm gneiss' εHf and $\delta^{18}O$ values. The Sabot amphibolite has εHf values ranging from +9.0 to +12.3. There are two different oxygen populations – the cluster of points between 8.17‰ and 9.33‰ and the lone point at 5.57‰, which is within the band of mantle values.

Figure 14 compares the maximum and minimum depleted mantle model ages of the magma to the crystallization age of the rock. The black line is a 1:1 reference line. If the rock crystallized at the time the magma separated from the depleted mantle, it would plot on the 1:1 line. The State Farm gneiss' range plots well above the reference line, as does the maximum model age of the Montpelier anorthosite. At 1000Ma, granitoid A plots above the line, within the large range of model ages of granitoid B, whose minimum model age is beneath the reference line. At 620Ma, granitoid B plots with the range of granitoid A, which is above the reference line. The Sabot amphibolite's maximum and minimum model ages are not far apart and plot close to the reference line.

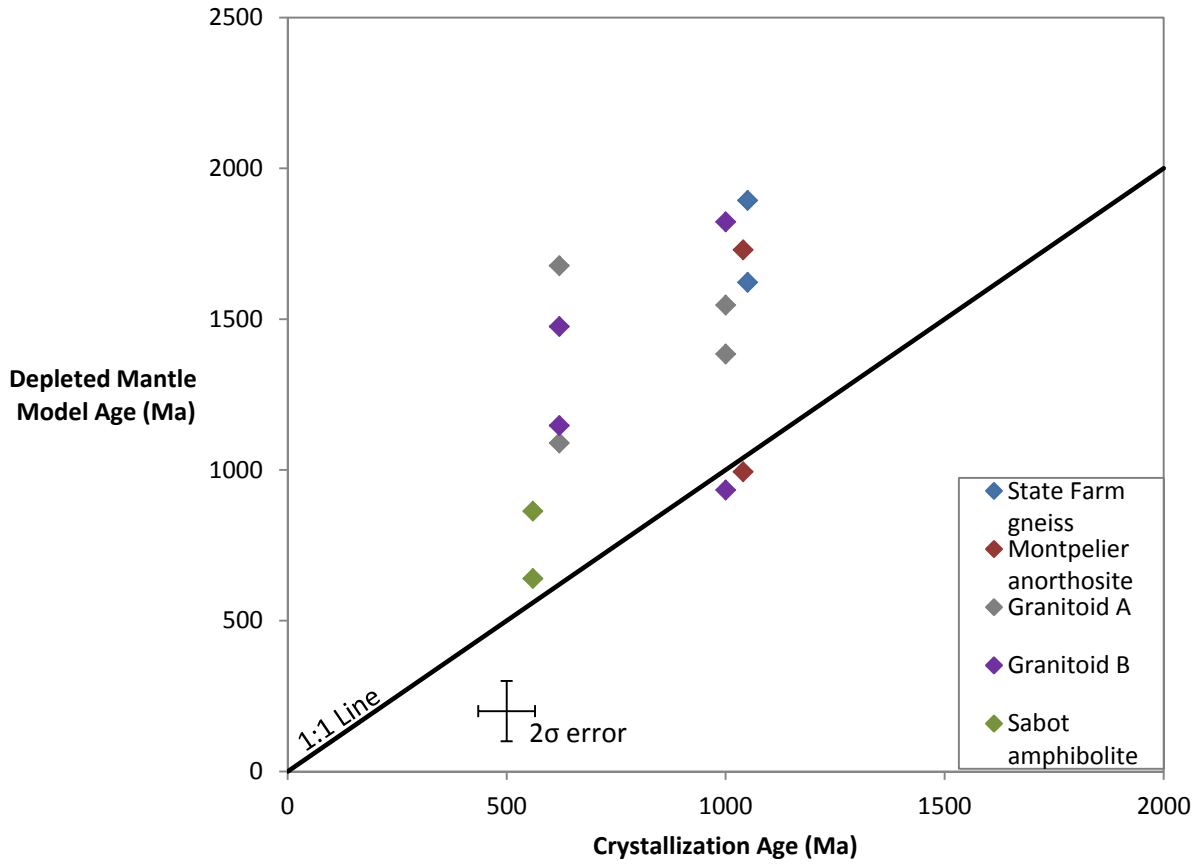

Figure 14. Graph of the depleted mantle model age compared to the crystallization age of the five rocks. The 1:1 reference line represents a rock that came out of the depleted mantle and crystallized shortly after.

Discussion

Sources of the Neoproterozoic granitoids

Figure 11, previously described in the 'Results' section, is a plot of the $\delta^{18}O$ data for the State Farm gneiss and the Neoproterozoic granitoids. The State Farm gneiss has values above 6.5‰, suggesting a supracrustal component in the magma. Granitoid A has tight range between 6‰ and 7‰ for the regions of the zircons that crystallized at 620Ma. The inherited cores and old parts range from 6.5‰ to 8.5‰. The lower values suggest a mantle like component, while the upper values suggest a supracrustal component in the magma. Granitoid B has a wide range from 1.5‰ to 6.5‰. Some of these values fall within mantle values, which could suggest a mantle like component. The values below 5.3‰ indicate the magma interacted with meteoric water at temperatures greater than 350°C. The oxygen isotope values suggest interactions of hydrothermally altered magma and a mantle sourced or supracrustal sourced magma. Either interaction would explain the <5.3‰ values and the range of values through mantle like components to about 6.5‰.

Figure 12 is a plot of $\delta^{18}O$ values versus εHf values at the time of crystallization of the granitoids. The State Farm gneiss data cluster around -8, as do four inherited zircon cores from the granitoids. These negative values are consistent with evolved crustal rocks that crystallized

before 620Ma. One inherited core from granitoid A plots at -3.8, which would make it less evolved than the two other inherited cores from granitoid A. This zircon core falls between the State Farm gneiss and the granitoids, which may suggest that the analysis picked up the inherited core and the ~620Ma overgrowth of the zircon. The $\delta^{18}O$ values are consistent with the nearby granitoid A inherited cores and the State Farm gneiss, suggesting all three groups had similar crustal components in their melt(s). Conversely, the two granitoid B points around -8 have much lower $\delta^{18}O$ values than the gneiss and the granitoid A cores. This suggests that these granitoid B cores formed around the same time as the gneiss and granitoid A cores, but came from a source that had been hydrothermally altered at temperatures greater than 350°C.

Two inherited zircon cores of granitoid A have εHf and $\delta^{18}O$ values consistent with the State Farm gneiss. These cores could have been inherited directly from the gneiss and incorporated into the magma that crystallized to form granitoid A. Two inherited cores from granitoid B have εHf values similar to the State Farm gneiss, but $\delta^{18}O$ values between 4.5 and 5‰. One explanation for this is that the cores are from the State Farm gneiss, interacted with the hydrothermally altered source of granitoid B, and were emplaced in granitoid B at 620Ma when the granitoid crystallized.

Most of the data for granitoids A and B plots vertically from around 0 up to about +5. Granitoid A is spread around 0ε, while granitoid B is spread between 0 and +5. This suggests the source of the granitoids had εHf values similar to CHUR or slightly more enriched in Hf. Positive values suggest that the source of the granitoids could have a component from melting of the depleted mantle. One outlier from granitoid B plots at -13.5 and around 2‰. The $\delta^{18}O$ value is consistent with other data from the granitoid, but, at -13.5, it is the most evolved grain on the graph.

Most of the εHf values for the Neoproterozoic granitoids are within a range from around 0εHf up to about +5. For the points within that range, the εHf values indicate that the granitoids had a different source that the gneiss. The granitoids' more positive εHf values are more juvenile than the gneiss's, so the granitoids would have needed a more juvenile source than the gneiss. This does not preclude mixing of a juvenile source and the State Farm gneiss.

The oxygen isotope data confirm a source other than the gneiss. The gneiss plots at about 7‰ or above. If the gneiss was the source of the inherited regions in the granitoids, those regions should have similar $\delta^{18}O$ values. Several points from granitoid A plot around 7‰ and several inherited cores plot above 7‰, but the rest of the data from the granitoids plots below.

The εHf values in combination with the $\delta^{18}O$ values suggest that the State Farm gneiss was not the sole source of the Neoproterozoic granitoids. The granitoids have a more juvenile εHf source and $\delta^{18}O$ values closer to the mantle than the gneiss. These data in part contradict past interpretations that the granitoids were formed from partial melting of the State Farm gneiss. The inherited cores in the granitoids have with very similar isotopic signatures to the gneiss, but the younger regions of the zircons have at least a juvenile component with low $\delta^{18}O$ values mixed with a supracrustal source.

Sources of the Sabot amphibolite

To evaluate the potential sources of the Sabot amphibolite, zircon isotope data was plotted for the gneiss, anothosite, granitoids, and amphibolite at 560Ma, when the amphibolite crystallized. Values for the amphibolite cluster around +11 and 8.7‰. The epsilon Hf values are close to the depleted mantle values, but the oxygen data suggests the introduction of a supracrustal component. A lone point plots at +9 and 5.57‰, which indicates a source with values close to the depleted mantle and oxygen values like the mantle. The location of this point

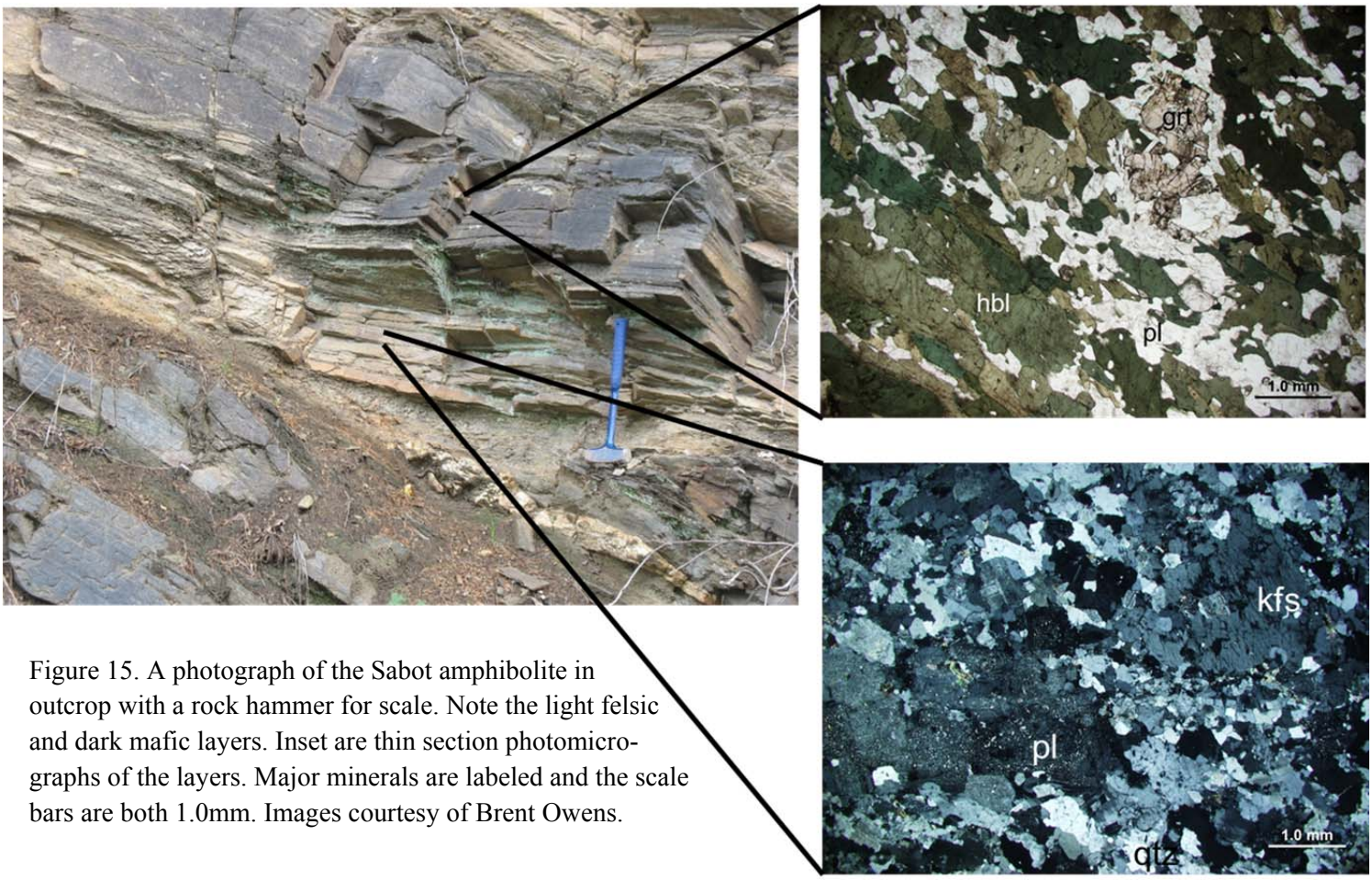

Figure 15. A photograph of the Sabot amphibolite in outcrop with a rock hammer for scale. Note the light felsic and dark mafic layers. Inset are thin section photomicrographs of the layers. Major minerals are labeled and the scale bars are both 1.0mm. Images courtesy of Brent Owens.

within the mantle oxygen parameters tentatively suggests that there were two different melts that formed the amphibolite or a range of oxygen values in one melt or melts.

Observations from the field and thin sections support a scenario with more than one melt. Interbedded layers of felsic and mafic material are seen in Figure R. The bulk composition of analyzed mafic layers ranges from basalts to basaltic andesites, while the bulk composition of one analyzed felsic layer is rhyolite. There are interpreted to be interbedded volcanic layers (Martin and Owens, 2012). The isotope data, though scarce, corroborates two different magma sources.

Sources of the Montpelier anorthosite

The Montpelier anothosite has few data points, so any conclusions are fairly speculative. One point has a very similar isotopic signature to the State Farm gneiss data, suggesting a similar source or magma (Fig. 13). It may also be possible, given the field relationships of the anorthosite and the gneiss (Fig. 2), that the anorthosite intruded the gneiss at depth and picked up its isotopic signature before crystallizing. It is also possible that this data is from a zircon xenocryst picked up from the host rock (the State Farm gneiss) of the anorthosite.

The other data points have positive εHf values and $\delta^{18}O$ values around 8‰. The εHf values are around +1.4, which suggest a juvenile source like the depleted mantle and not an evolved source like the State Farm gneiss (cluster around 9.75‰). The εHf values of the anorthosite are also isotopically similar to the Neoproterozoic granitoids. The $\delta^{18}O$ values around

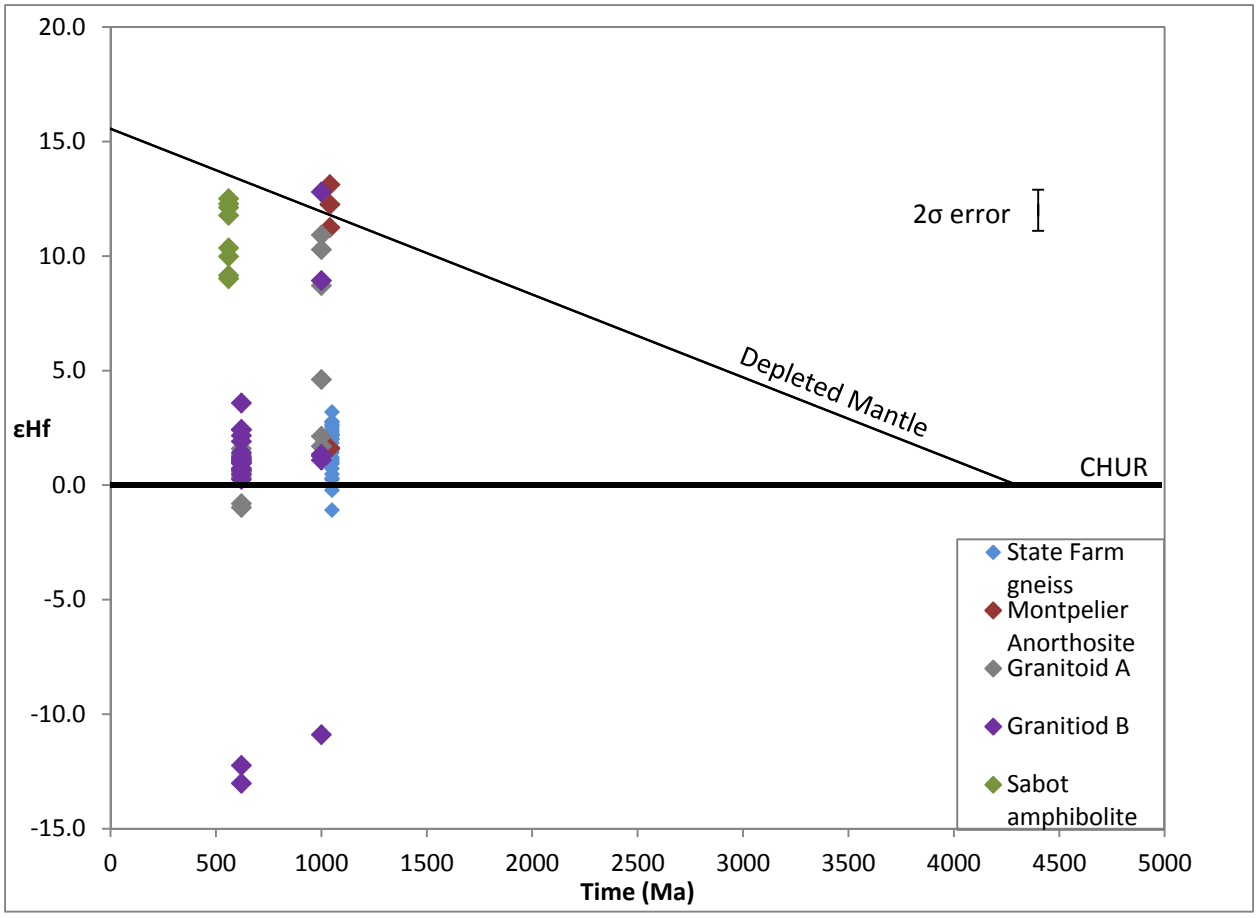

Figure 16. Graph of εHf values compared to time. The samples are plotted at the time of crystallization. CHUR values are marked at zero with the dark line. The depleted mantle in the graph separates from CHUR at 4300Ma.

8‰ are consistent with the State Farm gneiss and suggest a supracrustal component in the melt. Any further discussion of isotopic petrography is outside the scope of this paper.

Comparisons to the Depleted Mantle

Figure 16 is a graph of epsilon Hf compared to time and the evolution of the depleted mantle (DM). The State Farm gneiss and most of the points for granitoids A and B plot below the depleted mantle line, suggesting that there was a long time between the rocks' separation from the depleted mantle and their crystallization dates. One point for the anorthosite plots with the gneiss, but the other three points plot close to or above the depleted mantle, which tentatively suggests that the anorthosite had Hf concentrations very similar to the depleted mantle and crystallized soon after leaving the depleted mantle. Three points for granitoid A plot near the depleted mantle line and two points for granitoid B plot below and above the line. This suggests that these magma sources also had Hf concentrations similar to the depleted mantle and crystallized relatively soon after leaving that reservoir. The Sabot amphibolite plots close to the depleted mantle as well. These residence times are also seen in Figure 14, which compares model age with crystallization age.

Suggestions for Future Work

The results discussed in this paper warrant further investigation on two fronts. First, more data should be gathered for the Montpelier anorthosite. The four data points plotted here can suggest tentative relationships, but more data is needed to make firm statements. More zircon analyses would require a very large amount of crushed rock to gather a large zircon population to analyze. High precision analyses would be needed to avoid inclusions and pick up the low lead signatures. Repeating the U-Pb, Lu-Hf, and oxygen isotope analyses carried out in this paper would create a data set that might give clues to the source of the anorthosite. Anorthosite generation is poorly understood so more data from the Montpelier anorthosite could shed light on this.

Secondly, more data should be gathered for the Sabot amphibolite to explore the different magma sources for the mafic and felsic layers. Care should be taken to keep zircons from the layers separate. Zircons could also be gathered from any intermediate layers that have formed or the contacts between mafic and felsic layers. Careful sampling up the stratigraphic column could investigate variability between individual layers of mafic or felsic rock. Further work with Nd, Hf, and O isotopes could help determine the environment in which these layers formed.

Conclusions

The crystallization dates of the five rocks reflect a complex history of orogenic and rifting events starting during the Grenville orogeny and extending through the rifting of Rodinia.

The State Farm gneiss has an isotopic signature of a crustal source. The gneiss has negative εHf values and $\delta^{18}O$ values indicative of a supracrustal sourced melt. The gneiss crystallized during the Grenville orogeny, which would provide a setting for remelting of existing rocks at high pressures and temperatures.

The Neoproterozoic granitoids, which were thought to have formed from partial melting of the gneiss, have εHf and $\delta^{18}O$ values indicative of a mantle component in the source of the magma and mixing of a component that was hydrothermally altered at temperatures above 350˚C with a mantle or supracrustal component. High temperature hydrothermal alteration of the source is consistent with the past interpretation that the granitoids formed during a rifting event. Several inherited cores from granitoid A have very similar isotopic signatures to the State Farm gneiss, while several inherited cores from granitoid B have the same εHf values but $\delta^{18}O$ values that suggest a mantle component in the source of the melt. Some of the cores may have been inherited directly from the gneiss or formed from incorporated wall rock. The other cores with lower oxygen values are more mysterious.

The Montpelier anorthosite has low Pb concentrations, which made much of the data unusable. From the four data points collected, it can be tentatively suggested that the anorthosite has oxygen isotopic signatures very similar to the State Farm gneiss. One point has very similar εHf values and $\delta^{18}O$ values to the gneiss. This may be due to incorporation of wall rock as the anorthosite intruded the gneiss at depth, which would affect the isotopic signature of the magma, or a zircon xenocryst from the gneissthat was incorporated into the anorthosite. The three other data points have εHf values like the Neoproterozoic granitoids, suggesting that the anorthosite had a juvenile component in the magma source. These data are intriguing but should not be used to draw broader conclusions about anorthosite formation.

The Sabot amphibolite is composed of interbedded mafic and felsic layers. The zircon data provides evidence of two different sources for these melts. One source is likely the depleted mantle while the other had components of the depleted mantle and supracrustal material. The amphibolite is thought to have formed during final continental rifting. Additional analyses of the layers may reveal more detailed information about the sources of the layers. Further work should be completed to gather more data about the these rocks and the Goochland terrane as a whole to understand its history.

Acknowledgments

I would like to thank Dr. Martin, Dr. Piccoli, Chris Yakymchuk, Dr. Farquhar, and Dr. Rudnick for their invaluable advice and time. I would like to thank Dr. John Valley and his lab staff and Dr. Jeff Vervoort and his lab staff for the use of their machines and advice

Bibliography

Aleinikoff, J.N., Horton, J.W., and Walter, M., 1996, Middle Proterozoic age for Montpelier Anorthosite, Goochland terrane, eastern Piedmont, Virginia: Geological Society of America Bulletin, v. 108, no. 11, p. 1481-1491.

Appleby, S.K., Gillespie, M.R., Graham, C.M., Hinton, R.W., Oliver, G.J.H., Kelly, N.M., and EIMF, 2010, Do S-type granites commonly sample infracrustal sources?: New results from an integrated O, U-Pb and Hf isotope study of zircon: Contributions to Mineralogy and Petrology, v. 160, p. 115-132, doi: 10.1007/s00410-009-0469-3.

Bouvier, A., Vervoort, J.D., and Patchett, P.J., 2008, The Lu-Hf and Sm-Nd isotopic composition of CHUR: Constraints unequilibrated chondrites and implications for the bulk composition of terrestrial plants: Earth and Planetary Science Letters, v. 273, p. 48-57.

Bowring, S.A., and Schmitz, M.D., 2003, High-precision U-Pb zircon geochronology and the stratigraphic record, *in* Hanchar, J.M., and Hoskin, P.W.O., eds., Reviews in Mineralogy & Geochemistry: Zircon, vol. 53, p. 305-326.

Corfu, F., Hanchar, J.M., Hoskin, P.W.O., and Kinny, P., 2003, Atlas of zircon textures, *in* Hanchar, J.M., and Hoskin, P.W.O., eds., Reviews in Mineralogy & Geochemistry: Zircon, vol. 53, p. 468-500.

Dickin, A.P., 1997, Radiogenic Isotope Geology: Cambridge, Cambridge University Press, p. 225-234.

Eby, N., A-type Granitoids: http://faculty.uml.edu/nelson_eby/Research/A-type%20granites/A-type%20granites.htm (accessed November 2012).

Faure, G., 1986, Principles of Isotope Geochemistry: New York, John Wiley & Sons, ed. 2.

Griffin, W. L., Belousova, E. A., Shee, S. R., Pearson, N. J., & O'reilly, S. Y. (2004). Archean crustal evolution in the northern Yilgarn Craton: U–Pb and Hf-isotope evidence from detrital zircons. *Precambrian Research*, *131*(3), 231-282.

Hanchar, J.M., and Miller, C.F., 1993, Zircon zonation patterns as revealed by cathodoluminescence and backscattered electron images: Implications for interpretation of complex crustal histories: Chemical Geology, vol. 110, p. 1-13.

Hoskin, P.O., 2000, Patterns of Chaos: Fractal statistics and the oscillatory chemistry of zircon: Geochimica et Cosmochimica Acta, vol. 64, no. 11, p. 1905–1923.

Hoskin, P.O., and Schaltregger, U., 2003, The Composition of Zircon and Igneous and Metamorphic Petrogenesis, *in* Hanchar, J.M., and Hoskin, P.W.O., eds., Reviews in Mineralogy & Geochemistry: Zircon, vol. 53, p. 27-62.

Kemp, A.I.S., and Hawkesworth, C.J., Growth and differentiation of the continental crust from isotope studies of accessory minerals, *in* Rudnick, R.L., eds., The Crust, *in* Holland, H.D., and Turekian, H.H., Treatise on Geochemistry: Pergamon, Oxford, Elsevier, sec. 3.12 (in press).

Kinny, P.D., and Maas, R., 2003, Lu-Hf and Sm-Nd isotope systems in zircon, *in* Hanchar, J.M., and Hoskin, P.W.O., eds., Reviews in Mineralogy & Geochemistry: Zircon, vol. 53, p. 327-341.

Kita, N.T., Ushikubo, T., Bin, F., and Valley, J.W., 2009, High precision SIMS oxygen isotope analysis and the effect of sample topography: Chemical Geology, vol. 246, p. 43-57.

Martin, A.J., and Owens, B.E., 2012, Implications of c. 550 Ma crystallization of the Sabot amphibolite protolith in the Goochland terrane of the central Virginia Piedmont: Geological Society of America Abstracts with Program, vol. 44, no. 7, p.172.

Nesse, W.D., 2000, Introduction to Mineralogy: New York, Oxford University Press, p. 176-177, p. 313.

Owens, B.E., Buchwaldt, R., and Shirvell, C.R., 2010, Geochemical and geochronological evidence for Devonian magmatism revealed in the Maidens gneiss, Goochland terrane, Virginia, *in* Tollo, R.P., Bartholomew, M.J., Hibbard, J.P., and Karabinos, P.M., eds., From Rodinia to Pangea: The Lithotectonic Record of the Appalachian Region: Geological Society of America Memoir 206, p. 1–14, doi: 10.1130/2010.1206 (28).

Owens, B.E., and Samson, S.D., 2004, Nd isotopic constraints on the magmatic history of the Goochland terrane, easternmost Grenville crust in the southern Appalachians *in* Tollo, R.P., Corriveau, L., McLelland, J., and Bartholomew, M.J., eds., Proterozoic tectonic evolution of the Grenville orogen in North America: Boulder, Colorado, Geological Society of America Memoir 197, p. 601-608.

Owens, B.E., and Tucker, R.D., 2003, Geochronology of the Mesoproterozoic State Farm gneiss and associated Neoproterozoic granitoids, Goochland terrane, Virginia: Geological Society of America Bulletin, v. 115, no. 8, p. 972-982, doi: 2003107.

Parrish, R.R., and Noble, S.R., 2003, Zircon U-Th-Pb geochronology by isotope dilution-thermal ionization mass spectrometry (ID-TIMS), *in* Hanchar, J.M., and Hoskin, P.W.O., eds., Reviews in Mineralogy & Geochemistry: Zircon, vol. 53, p. 183-213.

Poller, U., Huth, J., Hoppe, P., and Williams, I.S., 2001, REE, U, Th, and Hf Distribution in Zircon from Western Carpathian Variscan granitoids: A combined cathodoluminesence and ion microprobe study: American Journal of Science, vol. 301, p. 858-876.

Scherer, E., Münker, C., and Mezger, K., 2001, Calibration of the lutetium-hafnium clock: Science, v. 293, p. 683–687.

Tollo, R.P., Corriveau, L., McLelland, J., and Bartholomew, M.J., 2004, Proterozoic tectonic evolution of the Grenville orogen in North America: An introduction, *in* Tollo, R.P., Corriveau, L., McLelland, J., and Bartholomew, M.J., eds., Proterozoic tectonic evolution of the Grenville orogen in North America: Boulder, Colorado, Geological Society of America Memoir 197, p. 1-18.

Valley, J.W., 2003, Oxygen Isotopes in Zircon, *in* Hanchar, J.M., and Hoskin, P.W.O., eds., Reviews in Mineralogy & Geochemistry: Zircon, vol. 53, p. 343-385.

Vervoort, J.D, and Blichert-Toft, J., 1999, Evolution of the depleted mantle: Hf isotope evidence from juvenile rocks though time: Geochimica et Cosmochimica Acta, v. 63, is. 3-4, p. 533-556.

Appendix A.

I pledge on my honor that I have not given or received any unauthorized assistance or plagiarized on this assignment.

Rock	Maximum date (Ma)	Minimum date (Ma)	Average date (Ma)	Average 1 σ absolute error	Max. $\delta^{18}O$ (‰)	Min. $\delta^{18}O$ (‰)	Average $\delta^{18}O$ (‰)	Average 2 σ error	Max. $^{176}Hf/^{177}Hf$	Min. $^{176}Hf/^{177}Hf$	Average $^{176}Hf/^{177}Hf$	Average 2 σ error	Max. $^{176}Lu/^{177}Hf$	Min. $^{176}Lu/^{177}Hf$	Average $^{176}Lu/^{177}Hf$	Average 2 σ error
State Farm gneiss	1098.8	928.8	1028.6	32.6	9.69	6.93	7.78	0.14	0.282215	0.282098	0.282170	0.00002	0.00153	0.00021	0.00044	0.00002
Montpelier anorthosite	4927.3	1121.1	2332.0	123.9	8.40	7.60	8.06	0.26	0.282491	0.282166	0.282400	0.00003	0.00140	0.00004	0.00041	0.00001
Sabot amphibolite	608.0	501.9	560.9	44.1	9.33	5.57	8.30	0.21	0.282831	0.282698	0.282767	0.00004	0.00496	0.00083	0.00271	0.00013
Granitoid A												0.00003				0.00005
Inherited Cores	1100.3	940.9	1014.8	75.2	8.29	6.51	7.56	0.21	0.282407	0.282206	0.282283		0.00074	0.00032	0.00052	
Old Regions	977.8	939.7	961.5	125.9	6.86	6.65	6.76	0.28	0.282469	0.282456	0.282462		0.00074	0.00048	0.00061	
620Ma Regions	690.5	567.9	642.5	52.1	6.92	6.21	6.54	0.21	0.282454	0.282379	0.282423		0.00201	0.00042	0.00116	
Granitoid B												0.00004				0.00008
Inherited Cores	1109.4	965.0	1041.6	42.6	4.82	3.58	4.31	0.27	0.282466	0.282145	0.282267		0.00330	0.00051	0.00146	
Old Regions	1107.2	967.7	1027.2	45.3	4.91	1.78	2.81	0.28	0.282553	0.282533	0.282541		0.00294	0.00127	0.00184	
620Ma Regions	698.3	563.4	655.2	38.3	6.56	1.79	4.39	0.26	0.282568	0.282423	0.282469		0.00350	0.00067	0.00214	

Table 1. Maximum, minimum, and average data values for the five rocks. Granitoids A and B are subdivided by age.